ISSN 1070-3632, Russian Journal of General Chemistry, 2015, Vol. 85, No. 3, pp. 731–745. © Pleiades Publishing, Ltd., 2015.

Spectroscopic and Thermal Investigations of Charge-Transfer Complexes Formed between Cefotaxime Sodium Drug and Various Acceptors[1]

Mahmoud M. Ali[a], Akmal S. Gaballa[b], and Said M. Teleb[a]

[a] *Chemistry Department, Faculty of Science, Zagazig University, Zagazig, 44516 Egypt*

[b] *Faculty of Specific Education, Zagazig University, Zagazig, 44516 Egypt*

e-mail: akmalsg@yahoo.com; akmalsg@zu.edu.eg

Received February 1, 2015

Abstract—Charge-transfer complexes formed between cefotaxime sodium (CFX) as electron donor with different electron acceptors as iodine (I_2), picric acid (HPA), chloranilic acid (H_2CA), 2,3-dichloro-5,6-dicyano-1,4-benzoquinone (DDQ), and 7,7',8,8'-tetracyanoquinodimethane (TCNQ) have been studied in the liquid and solid states. The stoichiometries of all complexes were found to be 1 : 1 molar ratio between the donor (CFX) and acceptors (I_2, HPA, H_2CA, DDQ, and TCNQ). Characterizations of the formed CT-complexes were based on elemental analyses, photometric titration measurements, IR, and ^{1}H NMR spectra as well as thermal analyses. The characteristic physical constants (K_{CT}, ε_{CT}, μ, ΔG, I_D, f, E_{CT}) of the formed CT-complexes are shown to be strongly dependent on the type and structure of the electron acceptors. Finally, the biological activities of the obtained CT complexes were tested for their antibacterial activities.

Keywords: charge transfer, cefotaxime, I_2, HPA, H_2CA, DDQ, TCNQ, UV-visible, IR, ^{1}H NMR, TGA, DTG spectrometry

DOI: 10.1134/S1070363215020322

INTRODUCTION

Over the last few decades, there has been a great importance of the charge transfer in chemical reactions, including addition, substitution, condensation [1, 2], biochemical, bioelectrochemical energy-transfer processes [3], biological systems [4] and drug–receptor binding mechanisms [5]. Certain π-acceptors have been successfully utilized in the pharmaceutical analysis of some drugs in the pure form or in pharmaceutical preparations [6–12]. Charge-transfer complexation is very important in many applications and fields such as non-linear optical materials, electrically conductive materials [13–16], second-order non-linear optical activity [17], micro emulsions, surface chemistry [18], photocatalysts [19], dendrimers [20], solar energy storage [21], organic semiconductors [22], and the investigation of redox processes [23]. Charge-transfer complexes that use organic species are intensively studied because of their special type of interaction, which is accompanied by the transfer of an electron from the donor to the acceptor [24, 25]. In addition, the protonation of the donor from acidic acceptors is a route for the formation of ion-pair adducts [26–28]. In general, the charge-transfer complexation can simply depend on the ionization potential of the donor and the electron affinity of the acceptor [29–31].

Cefotaxime sodium, chemically is sodium (6R,7R)-7-[(*Z*)-2-(2-amino-4-thiazolyl)-2-(methoxyimino)acetamido]-3-acetyl-oxymethyl-3-cephem-4-carboxylate [32] and is a third-generation of cephalosporin. Cephalosporin is antibacterial used in the treatment of infections due to susceptible gram-positive and gram-

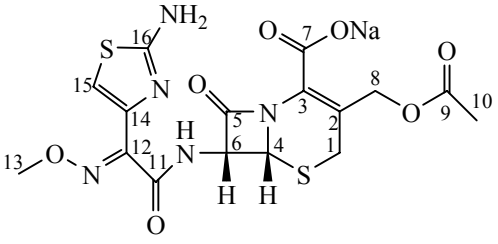

Scheme 1. Structure of cefotaxime sodium (CFX).

[1] The text was submitted by the authors in English.

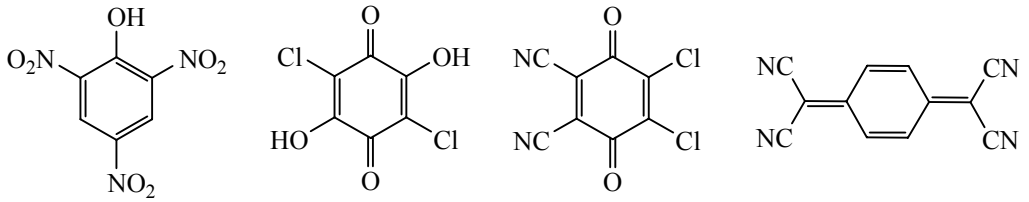

Scheme 2. Structure of the acceptors.

negative bacteria, including infections of the abdomen, bone, joints, central nervous system, skin structure, genitourinary tract, respiratory tract and in early Lyme disease [32–36].

To continue our interest in studying the synthesis and spectroscopic characterization of various CT-complexes in order to understand the nature of their CT-interaction [37, 38], we have investigated the CT interaction of the drug (cefotaxime sodium, CFX) as an electron donor with various electron acceptors (I_2.HPA, H_2CA, DDQ, TCNQ),

The nature and structure of the final products have been characterized using elemental analyses, electronic absorption spectroscopy, IR, ^{1}H NMR, and thermal analyses.

EXPERIMENTAL

Chemicals and spectral measurements. All chemicals used were of a high grade. The compound (cefotaxime sodium, CFX) was obtained from Sigma–Aldrich Chemical Co., USA with purity of > 99.00% and was used without a further purification. Iodine (I_2), picric acid (HPA) chloranilic acid (H_2CA), 2,3-dichloro-5,6-dicyano-*p*-benzoquinone (DDQ), and 7,7',8,8'-tetracyanoquinodimethane (TCNQ) purchased from Merck Chemical Co. and were also used as received.

The electronic absorption spectra were recorded in region of 200–900 nm using UV-Vis. Spectrophotometer model JASCO V-530 with quartz cell of 1.00 cm path length. The infrared spectra of the reactants and the obtained complexes were recorded using KBr discs on Perkin-Elmer 1430 ratio recording Infrared spectrometer. ^{1}H NMR spectra were recorded on Varian spectrophotometer Brucker 400 operating at 400 MHz using dimethylsulphoxide-d_6 as a solvent and TMS as the internal reference.

Elemental analyses of the dried and pure samples were carried out in the microanalysis unit of Cairo University, Egypt using CHNS-932 (LECO) and Vario Elemental analysers. Chlorine was determined by burning the substance in oxygen with platinum contact and following titration with mercuric nitrate towards diphenylcarbazide. The results of elemental analyses of the solid complexes were in consistence with stoichiometric ratios obtained from photometric titrations.

Thermal analyses (TG, DTG) were carried out using a Shimadzu TGA-50 H computerized thermal analysis system. The system includes a program which processes data from the thermal analyzer with the ChromotPac C-R3A. The rate of heating of the samples was kept at 10ºC/min. Sample masses 4.597, 3.477, 4.270, 3.119, 2.539, and 4.761 mg for CFX and its complexes **I–V**, respectively were analyzed under N_2 flow at 20 mL/min.

Spectrophotometric titration measurements. Photometric titrations at 291, 360, 354, 391, 305, 359, 455, and 838 nm were performed for the reactions between CFX and acceptors I_2, HPA, H_2CA, DDQ, TCNQ, respectively in methanol at 25ºC using a Helios Gamma Unicam UV-Vis. Spectrophotometer and Jenway Visible range spectrophotometer model 6300 as follows. A 0.25, 0.50, 0.75, 1.00, 1.25, 1.5, 2.00, 2.50, 3.00, and 3.50 mL aliquot of a standard solution (1.0×10^{-4} M) of each acceptor in MeOH was added to 1.00 mL of 1.0×10^{-4} M CFX, which was also dissolved in MeOH. The concentration of CFX (C_d^0) in the reaction mixture was maintained at 1×10^{-4} M, while the concentrations of the acceptors (C_a^0) were changed over a wide range of concentrations (0.25×10^{-4} M to 3.5×10^{-4} M) to produce solutions with an acceptor molar ratio that varied from 0.25 : 1.00 to 3.50 : 1.00. The stoichiometry of the molecular CT-complexes was obtained from the determination of the conventional spectrophotometric molar ratio according to the known method]39].

Preparation of the solid complexes. The solid $[(CFX)_2I]\cdot I_3$ (**I**), [(HCFX)(PA)] (**II**), [(HCFX)(HCA)] (**III**), [(CFX_{-H})(HDDQ)] (**IV**), and [(CFX_{-H})

(HTCNQ)] (**V**) complexes were prepared by adding a methanolic solution (20.0 mL) of the acceptors (1.00 mmol) to a methanolic solution (10.0 mL) of the donor CFX (1.00 mmol). The resultant dark brown, scarlet-yellow, dark violet, dark red and dark green solutions of complexes **I–V**, respectively, were stirred for about 2 h at room temperature then left overnight to separate the solid complexes. The precipitated complexes were filtrated off, washed with MeOH (3 × 0.5 mL) and dried in vacuo over $CaCl_2$.

$[(CFX)_2I]^+ \cdot I_3^-$ (I). ^{1}H NMR spectra (400 MHz, DMSO-d_6), δ, ppm: 2.03 s (3H, CH_3), 3.42 d (2H, CH_2), 3.90 s (3H, CH_3), 5.18 s (1H, C*H*), 5.05 d (2H, CH_2), 5.95 s (1H, C*H*), 6.84 s (1H, C*H*), 6.94 d (2H, NH_2), 9.79 s (1H, N*H*). Found, %: C 26.25, H 2.28, N 9.57, S 8.75 . $C_{32}H_{32}I_4N_{10}Na_2O_{14}S_4$. Calculated, %: C 26.28, H 2.21, N 9.58, S 8.77. *M* 1462.51.

[(HCFX)(PA)] (II). ^{1}H NMR spectra (400 MHz, DMSO-d_6), δ, ppm: 2.03 s (3H, CH_3), 3.32 d (2H, CH_2), 3.83 (s, 3H, CH_3), 4.92 s (1H, C*H*), 4.72 d (2H, CH_2), 5.21 s (1H, C*H*), 6.78 s (1H, C*H*), 7.34 d (3H, NH_3^+), 8.59 s (2H, $H^{3,5}$, PA), 9.54 s (1H, N*H*). Found, %: C 37.26, H 2.86, N 15.84, S 9.04. $C_{22}H_{19}N_8NaO_{14}S_2$. Calculated, %: C 37.40, H 2.71, N 15.86, S 9.08. *M* 706.55.

[(HCFX)(HCA)] (III). ^{1}H NMR spectra (400 MHz, DMSO-d_6), δ, ppm: 2.04 s (3H, CH_3), 3.22, 3.45 ABq (2H, CH_2), 3.84 s (3H, CH_3), 4.77 s (1H, C*H*), 5.00 d (2H, CH_2), 5.77 s (1H, C*H*), 6.75 s (1H, C*H*), 7.31 d (3H, NH_3^+), 9.59 s (1H, N*H*), 9.27 s (H, O*H*). Found, %: C 38.25, H 2.76, N 10.16, S 9.32. $C_{22}H_{18}Cl_2N_5NaO_{11}S_2$. Calculated, %: C 38.49, H 2.64, N 10.20. S 9.34. *M* 686.43.

[(CFX_{-H})(HDDQ)] (IV). ^{1}H NMR spectra (400 MHz, DMSO-d_6), δ, ppm: 1.98 s (3H, CH_3), 3.20 d (2H, CH_2), 3.83 s (3H, CH_3), 4.66 s (1H, C*H*), 5.04 d (2H, CH_2), 5.12 s (1H, NH^+), 5.82 s (1H, C*H*), 6.74 s (1H, C*H*), 9.66 s (1H, N*H*). Found, %: C 40.62, H 2.52, N 12.92, S 9.23. $C_{24}H_{16}Cl_2N_7NaO_9S$. Calculated, %: C 40.92, H 2.29, N 13.92, S 9.10. *M* 754.45.

[(CFX_{-H})(HTCNQ)] (V). ^{1}H NMR spectra (400 MHz, DMSO-d_6): δ, ppm: 2.02 s (3H, CH_3), 3.54, 3.61 ABq (2H, CH_2), 3.89 s (3H, CH_3), 4.71 s (1H, C*H*), 5.01 d (2H, CH_2), 5.17 s (1H, NH^+), 5.78 s (1H, C*H*), 7.22,7.32 d (4H, $H_{2,6}$, $H_{3,5}$, TCNQ), 6.84 s (1H, C*H*), 9.69 s (1H, N*H*). M 681.63. Found, %: C 49.25, H 3.21, N, 18.41, S 9.46. Calculated, %: C 49.34, H 2.96, N 18.49, S 9.41. *M* 681.63

Antibacterial activity. The antimicrobial activities of the newly synthesized CT complexes and the pure solvent were tested *in vitro* against Bacterial strains (*Pseudomonas aeruginosa, Staphylococcus aureous, Bacillus subtillis, Escherichia coli*) using agar well diffusion method. The samples were dissolved in DMSO to make a concentration of 100 μg/mL. The inoculum (1×10^8 Cfu/mL) was added to molten agar and the media were shaken to disperse the microorganisms. Four millimeters diameter wells were punched in the agar with a sterile cork borer. A 10 mL of the sample was introduced in the well. Anti-microbial activity was evaluated by measuring the diameter of inhibition zone in mm. The experiments were conducted in triplicate [40, 41].

RESULTS AND DISCUSSION

Electronic spectra. Electronic absorption spectra of the donor CFX and of the formed CT-complexes are shown in Fig. 1. These spectra have revealed new strong absorption bands attributed to the CT-interactions. These bands are not present in the spectra of the free reactants and are observed at 291,354 ,360 , ,391) 305, 359, 455, and 838 nm for the complexes, $[(CFX)_2I]\cdot I_3$ (**I**), [(HCFX)(PA)] (**II**), [(HCFX)(HCA)] (**III**), [(CFX_{-H})(HDDQ)] (**IV**), and [(CFX_{-H})· (HTCNQ)] (**V**), respectively. The appearance of two absorption bands in the electronic spectrum of the iodine complex **I** are well known to be characteristic for the formation of polyiodide ion (I_n, n = 3, 5, 7) [42].

Photometric titration measurements based on these characteristic CT-absorption bands of the CT-complexes (Fig. 2) confirmed the complex formation in a ratio, CFX: acceptor of 1 : 1 in all cases. Here, we indicated that the observed relative low CFX acceptor molar ratios compared with those known for other related donor-acceptor systems could be attributed to the relatively high sterric effects of the systems under investigations [43]. The obtained spectrophotometric data (Tables 1 and 2) were used to calculate the values of both equilibrium constants, K_{CT}, and extinction coefficient, ε of the CT-complexes in MeOH for $[(CFX)_2I]\cdot I_3$, [(HCFX)(PA)], [(HCFX)(HCA)], [(CFX_{-H})· (H_2DDQ)] and [(CFX_{-H})(HTCNQ)] complexes based on the known Eq. (1) for the 1 : 1 stoichiometry]44].

$$\frac{C_d^0 C_a^0}{A} = \frac{1}{\varepsilon K_c} + \frac{C_d^0 + C_a^0}{\varepsilon}, \quad (1)$$

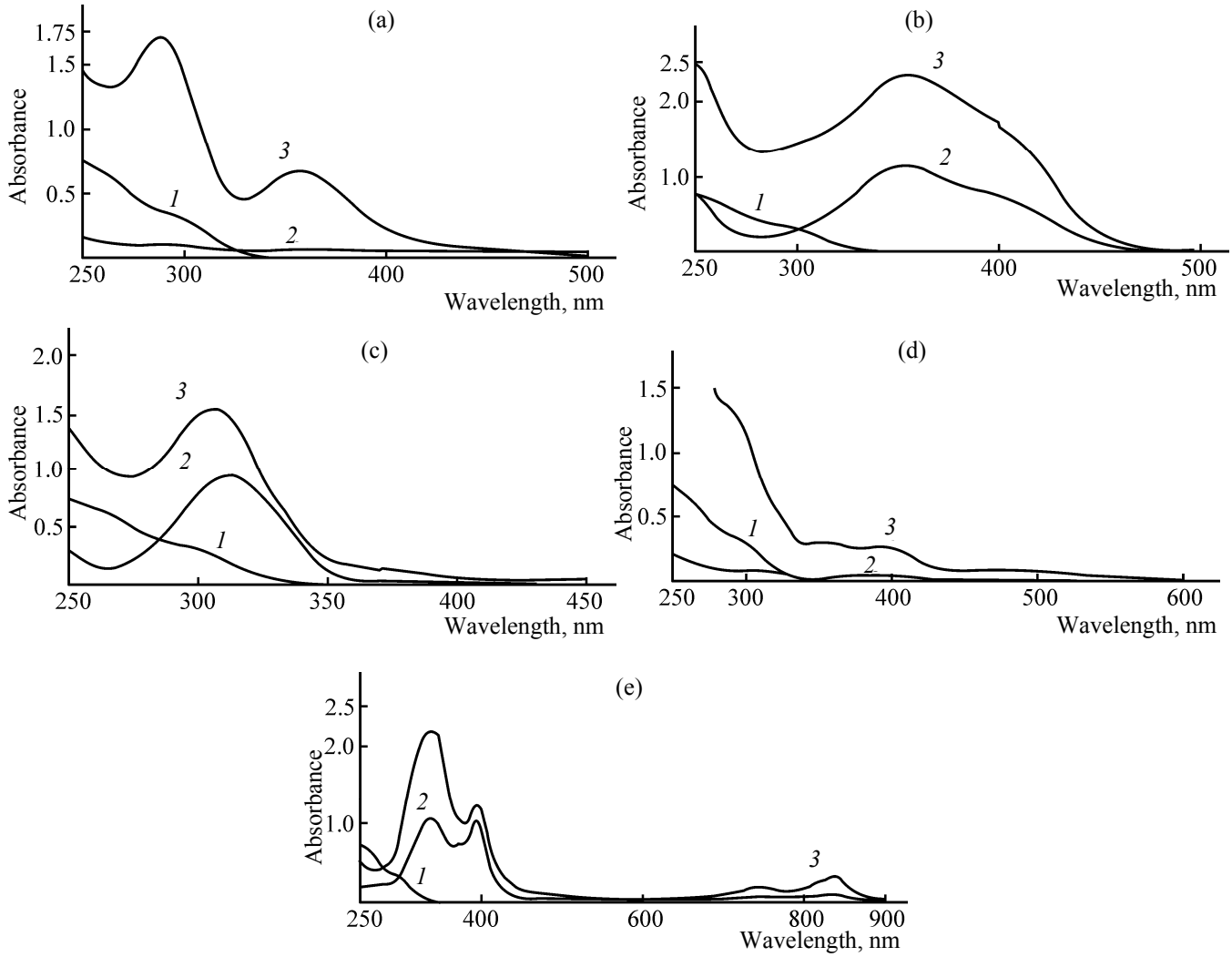

Fig. 1. Elecectronic absorption of (a) : CFX-I_2 reaction in MeOH {(*1*) [CFX] = 1×10^{-4} M, (*2*) [I_2] 1×10^{-4}, and (*3*) [CFX-I_2 product] = 1×10^{-4} M}; (b) CFX-HPA reaction in MeOH {(*1*) [CFX] = 1×10^{-4} M, (*2*) [HPA] = 1×10^{-4} M, and (*3*) [CFX-HPA product] = 1×10^{-4} M}; (c) CFX-H_2CA reaction in MeOH {(*1*) [CFX] = 1×10^{-4} M, (*2*) [H_2CA] = 1×10^{-4} M, and (*3*) [CFX-H_2CA product] = 1×10^{-4} M}; (d) CFX-DDQ reaction in MeOH {(*1*) ([CFX] = 1×10^{-4} M, (*2*) [DDQ] = 1×10^{-4} M, and (*3*) [CFX-DDQ product] = 1×10^{-4} M}; (e) CFX-TCNQ reaction in MeOH {(*1*) ([CFX] = 1×10^{-4} M, (*2*) [TCNQ] = 1×10^{-4} M, and (*3*) [CFX-TCNQ product] = 1×10^{-4} M}.

where C_a^0 and C_d^0 are initial concentration of the acceptor (I_2, HPA, H_2CA, DDQ, TCNQ) and donor CFX, respectively. *A* is the absorbance of new strong bands at (291, 360), (354, 391), (305), (359), (455, 838) nm. When. $C_a^0 C_d^0/A$ are plotted against $(C_a^0 + C_d^0)$, a straight line is obtained with a slope of $1/\varepsilon$ and intercept of $1/\varepsilon K_c$.

Some spectroscopic and physical parameters such as standard free energy (ΔG^0), transition dipole moment (μ), oscillator strength (*f*) and the ionization potential (I_D) were estimated for complexes dissolved in MeOH at 25ºC and summarized in Table 3.

The oscillator strength (*f*) is a dimensionless quantity used to express the transition probability of the CT band. From the CT absorption spectra, the oscillator strength (*f*) can be estimated by Eq, (2) [45].

$$f = 4.319 \times 10^{-9} (\varepsilon_{max\Delta} \nu_{1/2}), \quad (2)$$

where ε_{max} is the maximum extinction coefficient of the CT band, and $\Delta\nu_{1/2}$ is the half-bandwidth in cm^{-1} (i.e., the bandwidth at half of the maximum extinction coefficient value).

The transition dipole moments (μ) of the CFX CT-complexes have been calculated from equation 3 [46].

Table 1. The values of $C_a^0C_d^0$ and $C_a^0 + C_d^0$ for complex**es I** and **II.** C_d^0 is 1.00×10^{-4} M in all systems

$C_a^0 \times 10^{-4}$	Ratio a : d	$C_a^0 + C_d^0 \times 10^{-}$	$C_a^0C_d^0 \times 10^{-8}$	Complex **I**				Complex **II**			
				A	$C_a^0C_d^0/A$	A	$C_a^0C_d^0/A$	A	$C_a^0C_d^0/A$	A	$C_a^0C_d^0/A$
				291	$\times 10^{-8}$	360	$\times 10^{-8}$	354	$\times 10^{-8}$	391	$\times 10^{-8}$
0.25	0.25	1.25	0.25	0.099	2.525	0.034	7.352	0.14	1.700	0.146	1.712
0.50	0.50	1.50	0.50	0.176	2.840	0.078	6.410	0.31	1.600	0.202	2.475
0.75	0.75	1.75	0.75	0.284	2.640	0.129	5.813	0.40	1.847	0.304	2.467
1.00	1.00	2.00	1.00	0.351	2.849	0.182	5.490	0.49	2.016	0.367	2.724
1.25	1.25	2.25	1.25	0.385	3.246	0.214	5.841	0.51	2.450	0.391	3.196
1.50	1.50	2.50	1.50	0.394	3.836	0.243	6.170	0.53	2.824	0.382	3.926
2.00	2.00	3.00	2.00	0.455	4.395	0.308	5.763	0.54	3.690	0.417	4.796
2.50	2.50	3.50	2.50	0.498	5.020	0.347	7.204	0.54	4.612	0.418	5.980
3.00	3.00	4.00	3.00	0.523	5.736	0.372	8.064	0.55	5.454	0.422	7.109
3.50	3.50	4.50	3.50	0.632	5.537	0.391	8.950	0.56	6.250	0.424	8.254

Table 2. The values of $C_a^0C_d^0$ and $C_a^0 + C_d^0$ for complexes **III–V.** C_d^0 is 1.00×10^{-4} M in all systems

$C_a^0 \times 10^{-4}$	Ratio a : d	$C_a^0 + C_d^0 \times 10^{-4}$	$C_a^0C_d^0 \times 10^{-8}$	Complex **III**		Complex **IV**		Complex **V**			
				A	$C_a^0C_d^0/A$	A	$C_a^0C_d^0/A$	A	$C_a^0C_d^0/A$	A	$C_a^0C_d^0/A$
				305	$\times 10^{-8}$	359	$\times 10^{-8}$	455	$\times 10^{-8}$	838	$\times 10^{-8}$
0.25	0.25	1.25	0.25	0.062	4.03	0.064	3.900	0.089	2.800	0.044	5.68
0.50	0.50	1.50	0.50	0.142	3.52	0.105	4.760	0.182	2.740	0.121	4.13
0.75	0.75	1.75	0.75	0.174	4.31	0.161	4.650	0.253	2.964	0.180	4.14
1.00	1.00	2.00	1.00	0.221	4.52	0.212	4.716	0.318	3.144	0.219	4.56
1.25	1.25	2.25	1.25	0.228	5.48	0.231	5.411	0.324	3.858	0.232	5.38
1.50	1.50	2.50	1.50	0.239	6.27	0.272	5.510	0.329	4.559	0.263	5.70
2.00	2.00	3.00	2.00	0.242	8.26	0.289	6.920	0.336	5.952	0.278	7.19
2.50	2.50	3.50	2.50	0.243	10.28	0.302	8.278	0.348	7.183	0.293	8.53
3.00	3.00	4.00	3.00	0.246	12.19	0.331	9.063	0.378	8.356	0.346	8.67
3.50	3.50	4.50	3.50	0.248	14.11	0.352	9.943	0.412	9.485	0.378	9.25

$$\mu_{Debye} = 0.958 \left(\frac{\varepsilon_{max} \Delta \nu_{1/2}}{\nu_{max}} \right)^{1/2}. \quad (3)$$

The transition dipole moment can be used to determine if a particular transition is allowed; the transition from a bonding π-orbital to an antibonding π*-orbital is allowed because the integral that defines the transition dipole moment is nonzero.

The ionization potentials (I_D) of the CFX donor in the CT complexes were calculated using the empirical equation (4) derived by Aloisi and Pignataro [47].

$$I_D \text{ (eV)} = 5.76 + 1.53 \times 10^{-4} \nu_{CT}, \quad (4)$$

where ν_{CT} is the wavenumber in cm^{-1} that corresponds to the CT band formed from the interaction between the donor and the acceptor. The electron-donating power of a donor molecule is measured by its ionization potential, which is the energy required to

Table 3. Spectrophotometric data for CFX CT-complexes in MeOH

Complex	λ_{max}, nm	K_c, L/mol	ε_{max}, L mol^{-1} cm^{-1}	E_{CT}, eV	f	μ	I_D, eV	ΔG^0 (25°C), J mol^{-1} K^{-1}
I	360	0.14×10^4	1.42×10^4	3.454	20.39	39.070	10.009	-1.65×10^4
	291	1.51×10^4	0.66×10^4	4.273	14.25	29.687	11.017	-3.13×10^4
II	354	6.66×10^4	0.54×10^4	3.513	2.70	14.249	10.082	-2.50×10^4
	391	22.70×10^4	0.44×10^4	3.180	2.37	31.768	9.670	-2.79×10^4
III	305	3.76×10^4	0.33×10^4	3.948	4.07	16.245	10.776	-2.39×10^4
IV	359	1.25×10^4	0.50×10^4	3.464	8.63	25.670	10.021	-2.14×10^4
V	455	12.50×10^4	0.40×10^4	3.712	21.59	39.207	10.327	-2.66×10^4
	838	0.75×10^4	0.66×10^4	1.483	19.00	58.170	7.585	-2.02×10^4

Table 4. Characteristic infrared frequencies (cm^{-1}) and tentative assignments for CFX and its CT-complexes

CFX	HPA	H_2CA	DDQ	TCNQ	Complex **I**	Complex **II**	Complex **III**	Complex **IV**	Com-plex **V**	Assignments
3431 br 3350 br	3433 br	3235 w	3442 w 3339 w		3350 m 3283 m	3540 w 3347 br 3250 br	3416 m.br 3265 br	3416 s.br	3425 s.br	ν(N–H), ν(O–H), H bonded ν(N$^+$–H); of NH_2
3259 s				3137 m.s		3092 m	3265 m.br			ν(C–H), aromatic
2938 m 2822 m	2976 sh 2873 w			2969 w	2941w	2941 w	2948 m	2945 m	2941 m	ν_s(C–H) + ν_{as}(C–H)
			2243 m	2222 s				2224 m	2177 m	ν(C≡N), DDQ, TCNQ
1761 vs					1766 vs	1769 s	1778 m	1735 s	1743 s	ν(C=O), (lactam)
1728 s					1680 sh	1738 vs	1728 m	1670 s	1666 vs	ν(C=O), carboxylic ester
1648 vs		1665 s	1673 vs		1634 vs	1650 sh 1634 vs	1650 sh 1636 s	1636 s	1622 vs	ν(C=O), amide, quinone
	1607 vs					1558 vs				$\nu_{as}(NO_2)$
1536 vs	1347 m.s	1368 vs	1358 s	1542 s	1541m	1525 m	1536 vs	1565 m	1530 s	ν(C=C) stretch, ν(C=N) stretch
1388 m 1357 m					1385 w	1430 s 1339 s	1443 w m 1376	1444 s	1436 w 1378 w	ν(C–H) plane bending
1240 s	1316 m.s	1369 m	1268 ms	1352 m.s	1240 m	1275 s	1259 s	1267 s	1280 w	ν(C–N)
1043 s	1147 m.s	1290 vs	1216 w	1132 m.s	1039 s	1039 s	1046 m	1115 m	1237 w	ν(C–O)
	1083 m.s					1065 w				$\nu_s(NO_2)$, HPA
		856 m					843 m			ν(C–Cl)
728 w		690 m	796 s	861 s	735 v.w	739 w	758 w	664 w	811w	CH_2 rocking
	783 s 733 s									
562 v.w	698 s 646 sh	571 ms	615 s	473 vs	563 v.w	547 w	571 w	437 m	537 w	(C–H) out of plane
	550 m					433 w				δ(ONO): HPA

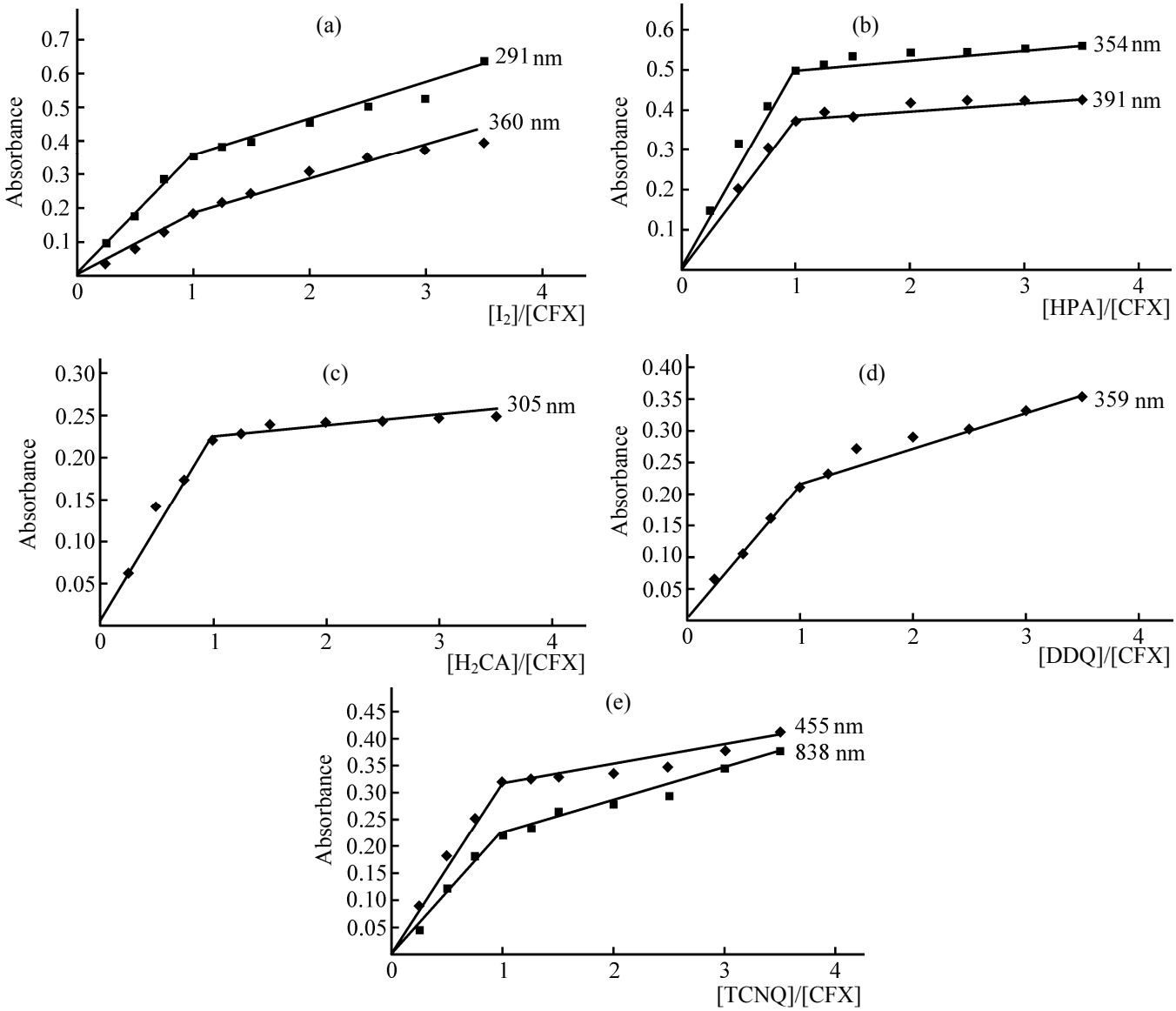

Fig. 2. Photometric titration curves of (a) CFX-I_2 reaction in MeOH at 291 and 360 nm; (b) CFX-HPA reaction in MeOH at 354 and 391 nm; (c) CFX-H_2CA reaction in MeOH at 305 nm; (d) CFX-DDQ reaction in MeOH at 359 nm; and (e) CFX-TCNQ reaction in MeOH at 455 and 838 nm.

remove electron from the highest occupied molecular orbital.

The energy values (E_{CT}) of the *n* to π* and π–π* interactions between the donor (CFX) and the acceptors were calculated using the equation derived by Briegleb equation (5) [48].

$$E_{CT} = (h\nu_{CT}) = 1243.667/\lambda_{CT}\ (\text{nm}), \quad (5)$$

where λ_{CT} is a wavelength of the CT band.

The standard free energy of complexation ΔG^0 for each complex was calculated using Eq. (6) [49].

$$\Delta G^0 = -2.303RT\log\ K_{CT}, \quad (6)$$

The obtained data in Table 3 showed that, the complexes $[(CFX)_2I]\cdot I_3$ and $[(CFX_{-H})(HTCNQ)]$ exhibit considerably higher values of both the oscillator strength (*f*) and the transition dipole moment (μ) which indicated a strong interaction between the donor–acceptor pairs with relatively high probabilities of CT transitions [50]. The obtained negative values of ΔG^0 for the CT-complexes indicate that the interaction between the drug and acceptors is exothermic and spontaneous [51, 52].

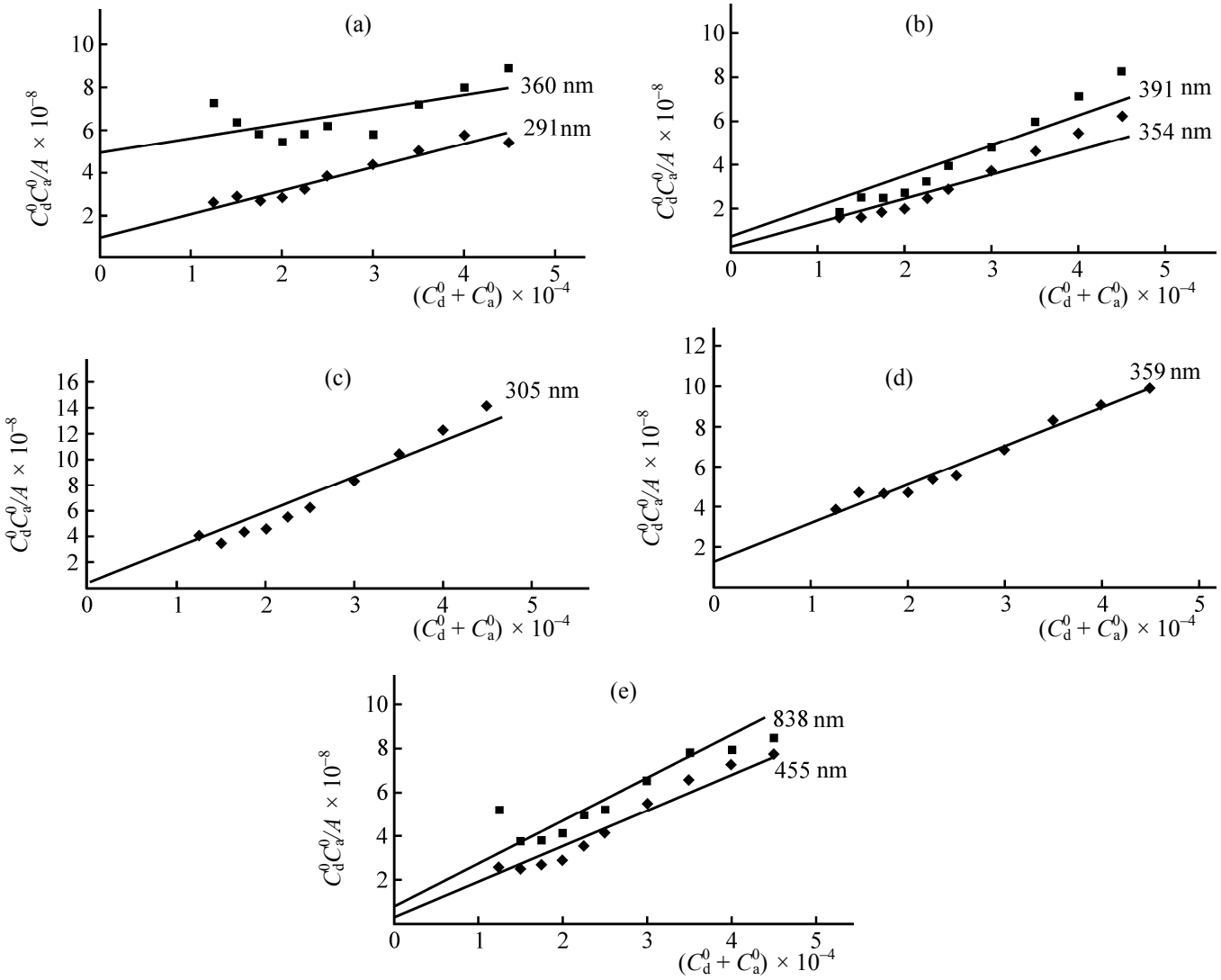

Fig. 3. Relation between $C_d^0C_a^0/A$ and $C_d^0 + C_a^0$ for (a) CFX-I_2 reaction in MeOH at 291 and 360 nm, (b) CFX-HPA reaction in MeOH at 391 nm and 354 nm, (c) CFX-H_2CA reaction in MeOH at 305 nm, (d) CFX-DDQ reaction in MeOH at 359 nm, and (e) CFX-TCNQ reaction in MeOH at 455 and 838 nm.

IR spectra. IR spectra of reactants and the obtained products are given in Fig. 4 and the assignments of their characteristic bands are given in Table 4. The formation of CT-complexes during the reaction of CFX with I_2, Picric acid, chloranilic acid, DDQ and TCNQ is strongly supported by observing of main infrared bands of the donor (CFX) and acceptors (HPA, H_2CA,DDQ, TCNQ) in the product spectra. However, the bands of the donor and acceptors in the complexes spectra reveal small shifts in wavenumber values and intensities compared with those of the free donor and acceptors. This should be attributed to the expected symmetry and electronic structure changes upon the formation of CT-complexes.

For the acid–base interaction, a proton transfer from the acceptor (acid) to the donor (base) is expected to occur. This seems to be liable to occur in the case of CFX interaction with picric and chloranilic acids. Such assumption is strongly supported as follow; the spectrum of free donor reveals to absorption peaks at 3431 and 3350 cm^{-1} with frequency difference equals to ~80 cm^{-1} which is characteristic to the presence of an $–NH_2$ group. Such absorption is not present any more in the spectra of complexes 2 and 3, but instead a medium intensity peaks are observed in the spectra of the two complexes at 3250 and 3265 cm^{-1}, respectively and are not present in the spectrum of the free donor. Such absorption could be attributed to the (N–H)

Table 5. ^{1}H NMR spectra (δ, ppm) for CFX and its CT-complexes in DMSO-d_6

Comp. no.	$C^{10}H_3$ CFX	C^1H_2 CFX	$C^{13}H_3$ CFX	C^4H CFX	C^8H_2 CFX	C^6H CFX	$C^{15}H$ CFX	NH_2 CFX	NH CFX	NH_3^+ CFX	$C{\equiv}N^+$-*H*	O*H* HCA	H_3/H_5 PA	$H_{2,3}/H_{6,5}$ TCNQ[a]
CFX	1.99	3.21 3.43	3.85	4.75	4.99	5.56	6.73	7.22	9.52	–				
I	2.03	3.42	3.90	5.18	5.05	5.95	6.84	6.94	9.79	–				
II	2.03	3.32	3.83	4.92	4.72	5.21	6.78	–	9.54	7.34			8.59	
III	2.04	3.22 3.45	3.84	4.77	5.00	5.77	6.75	–	9.59	7.31		9.27		
IV	1.98	3.20	3.83	4.66	5.04	5.82	6.74	–	9.66	–	5.12			
V	2.02	3.54 3.61	3.89	4.71	5.01	5.78	6.84	–	9.69	–	5.17			7.22, $H_{2,6}$ 7.32, $H_{3,5}$

[a] $H_{2,3}/H_{6,5}$ in free TCNQ observed at 9.06 s.

stretching vibration of hydrogen against positively charged nitrogen. We may suggest that, the acid-base interaction is associated with a proton migration followed by hydrogen bonding formation. The CFX–HPA and CFX–H_2CA interaction involves a protonation for the basic nitrogen of the CFX nitrogens. Accordingly, we may formulate the complex as $[(HCFX)^+(PA)^-]$, $[(HCFX)^+(HCA)^-]$. Due to the increased electron density on the picrate and chloranilate units as a result of charge transfer interaction and deprotonation of the acids upon complexation, the shift of $\nu_{as}(NO_2)$ of the picric acid and ν(C–Cl) of chloranilic acid to lower frequencies upon complexation can be attributed [53, 54].

The IR spectra of free DDQ and TCNQ show CN stretching frequencies at 2243 and 2222 cm^{-1}, respectively. The significant shift of these vibrations toward lower frequencies (2224 and 2177 cm^{-1}) on complexation is indicative of charge transfer from CFX to π of a C≡N group of DDQ and TCNQ which leads to a weakening of this bond. The C=O systems of the free donor go to lower frequencies upon complexation with DDQ and TCNQ and this is in consistence with the decreased electron density of the donor upon complexation [55, 56].

^{1}H NMR spectra. The ^{1}H NMR spectra of complexes present the persuasive confirmation of the complexation pathway by observing most of signals of the free reactants with some expected shift due to the changes in electronic density upon complexation. Thus, the ^{1}H NMR spectra of the CFX CT-complexes were measured in DMSO-d_6 at room temperature. The chemical shifts (δ) of the different types of protons of the CT complexes are summarized in Table 5.

The ^{1}H NMR spectrum of complex **I**, $[(CFX)_2I]^+{\cdot}I_3^-$ shows all of the signals of the donor but with small downfield shift compared with the corresponding spectrum of the free donor. This shift is expected and could be attributed to the decreased electron density of the donor upon complexation with iodine.

The spectrum of complex **II**, [(HCFX)(PA)[reveals a signal at 7.34 ppm, which is not detected in the spectrum of the free CFX donor, the integration of this signal is equivalent to 3 protons. The complex spectrum also shows the absence of the 11.94 ppm signal which is known to be characteristic for the phenolic proton of picric acid. Together, these data indicate that the amino and phenolic groups are involved in the formation of the CT complex between CFX and HPA and the complexation is associated with a proton transfer from the acid to the donor i.e. protonation of the amino group [57].

The ^{1}H NMR spectrum of the free chloranilic acid reveals a signal at 9.15 ppm due to the two phenolic protons [58, 59]. In the complex spectrum of [(HCFX)·(HCA)] (**III**), a signal at 9.27 ppm corresponding to one phenolic proton is observed. Furthermore, the complex spectrum shows a new signal at 7.31 ppm. This signal corresponds to 3 protons and does not exist in the spectrum of the free donor. This suggests that one of the acid phenolic protons is transferred to protonate the amino group of the donor.

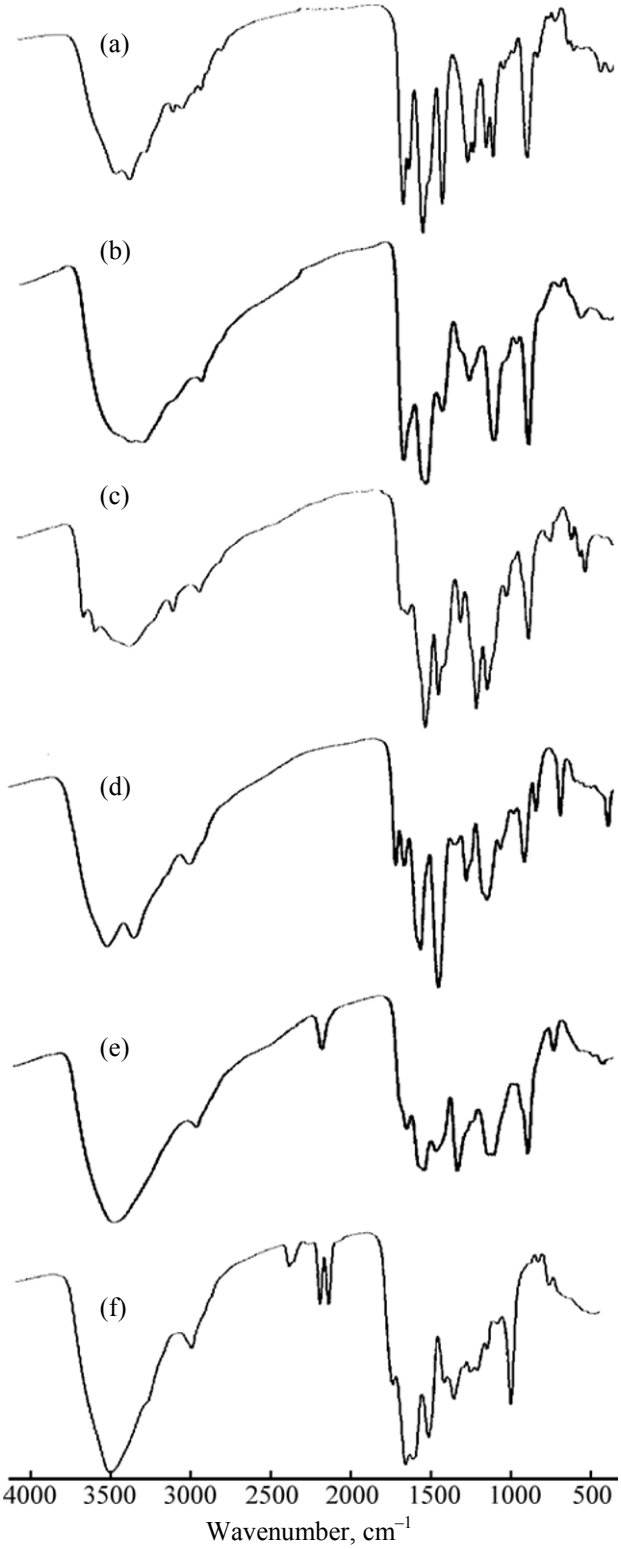

Fig. 4. Infrared spectra of (a) CFX donor and its CT-complexes (b) **I,** (c) **II,** (d) **III,** (e) **IV,** and (f) **V.**

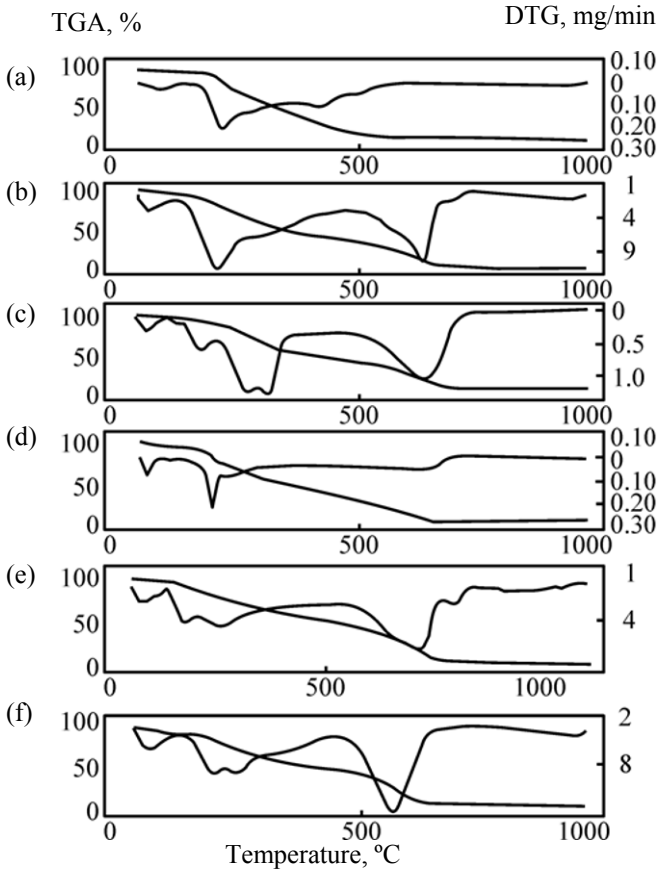

Fig. 5. Thermogravimetric (TGA) and derivative (DTG) of (a) CFX and its complexes (b) **I,** (c) **II,** (d) **III,** (e) **IV,** and (f) **V.**

The spectra of complexes **IV** and **V** show most of signals due to the reactants in clear evidence supporting its formation. The complex spectra show the absence of any signals due to $–NH_2$ group at 7.22 ppm as reflected by the spectrum of cefotaxime sodium (the free donor), but instead a new signal at 5.12 and 5.17 ppm for [($CFX_{–H}$)(HDDQ)] (**IV**) and [($CFX_{–H}$)(HTCNQ)] (**V**), respectively. We may suggest a proton transfer associated with the complex formation, but in this case from the donor to acceptor. One proton of $–NH_2$ group is transferred to a cyano group of DDQ and TCNQ to give $–C{\equiv}N^{+}–H$ and the complexes formula may be suggested to be [$(CFX_{–H})^{–}$·$(HDDQ)^{+}$] and [$(CFX_{–H})^{–}(HTCNQ)^{+}$] [59, 60].

Thermal analysis. The proposed structures for the complexes under investigation were confirmed by measuring TGA, and DTG thermograms (Fig. 5) under nitrogen flow. The thermal data obtained for complexes **I–V** together with the free donor, CFX are summarized and given in Table 6.

Table 6. The maximum temperature values for the decomposition along with the species lost in each step of the decomposition reaction of the free CFX and its CT-complexes

Complex	Decomposition	T_{max}, °C	Lost species	Weight loss, %	
				Found	Calculated
CFX	First stage	217 429 507	$C_{16}H_{16}N_5O_5S_2$	86.82	88.49
	Residue		NaO_2	10.50	11.51
I	First main stage	201 288	$C_{32}H_{32}N_{10}O_{10}S_4$	56.25	57.77
	Second stage	639 710	I_4	34.42	34.71
	Residue		Na_2O_4	6.93	7.52
II	First stage	167 270 311	$C_{16}H_{17}N_5O_5S_2$	58.72	59.93
	Second stage	648	$C_6H_2N_3O_7$	31.80	32.28
	Residue		NaO_2	06.98	07.78
III	First step	196	$C_{16}H_{17}N_5O_5S_2$	60.38	61.69
	Second step	652	$C_6HCl_2O_4$	29.00	30.30
	Residue		NaO_2	07.97	08.01
IV	First stage	164 251	$C_{16}H_{15}N_5O_5S_2$	59.46	59.82
	Second stage	715 794	$C_8HCl_2N_2O_2$	31.23	32.37
	Residue		NaO_2	07.11	07.81
V	First stage	200 252	$C_{16}H_{15}N_5O_5S_2$	60.45	61.83
	Second stage	588	$C_{12}H_5N_4$	30.13	30.10
	Residue		NaO_2	07.02	08.07

The free CFX decomposes in three steps at 217, 429, and 507ºC. The total weight loss associated with these steps of decomposition is near to the theoretical calculation. The decomposition mode of the complexes under investigation occurs in a similar manner in which the most residues is due to the presence of sodium dioxide, NaO_2.

The decomposition reactions of complex **I** occur in two closed main stages. The first stage of decomposition occurs in two steps at 201 and 288ºC with a weight loss of 56.25% and the second stage at 639 and 710ºC with a weight loss of 34.42%. These values of weight loss may be due to the loss of CFX organic moiety and iodine in good agreement with the calculated values of 57.77 and 34.71%, respectively.

In complex **II**, the decomposition reactions occur in two main stages. The first stage of decomposition occur in there steps at 167, 270, and 311ºC with a weight loss of 58.72%. This value of weight loss may be due to the loss of HCFX organic moiety in agreement with the calculated value of 59.93%. The second stage of decomposition occurs in one step at

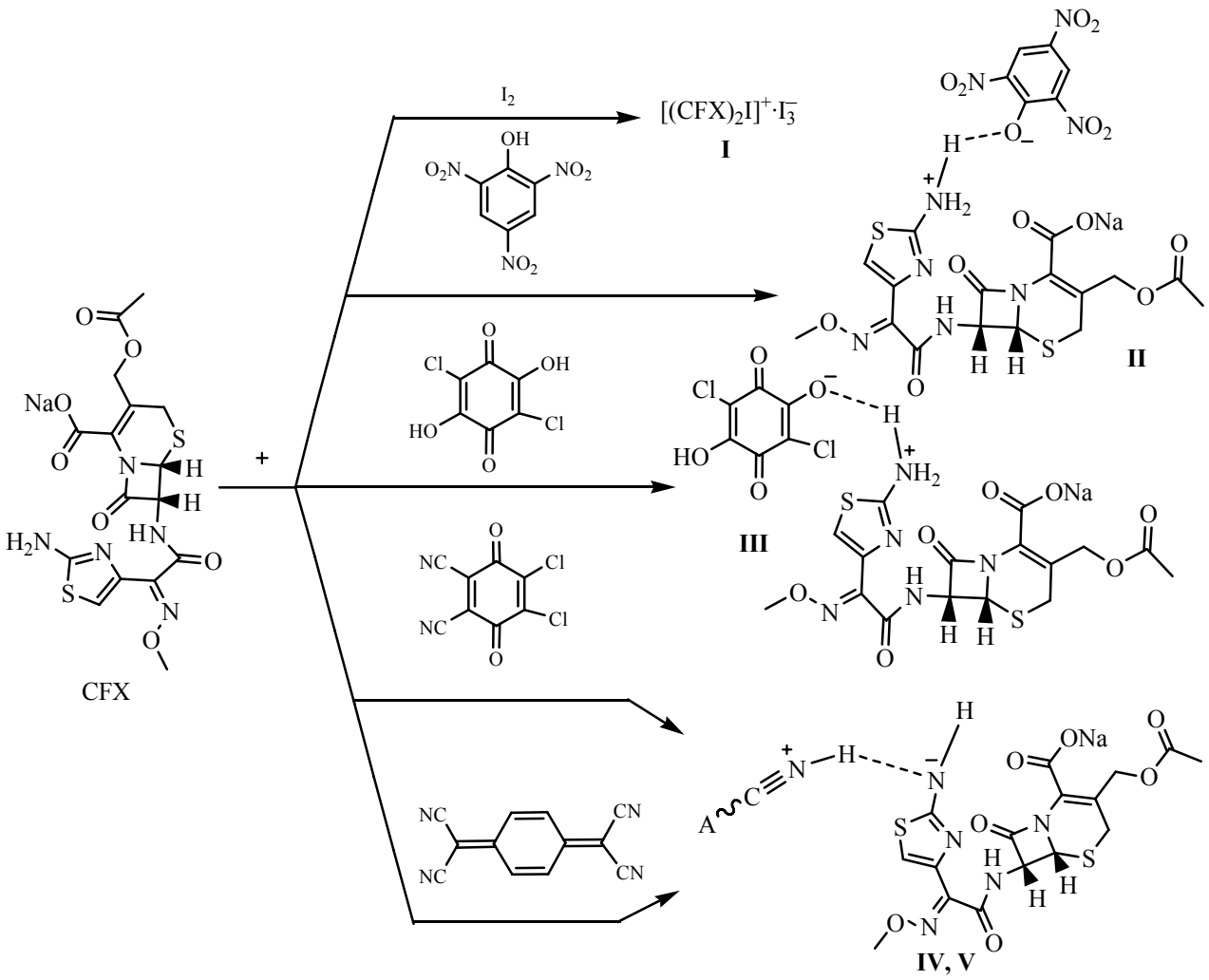

Scheme 3. Proposed CT-complexes of cefotaxime sodium (CFX) with different electron acceptors.

648ºC with a weight loss of 31.8%. This value of weight loss may be due to the loss of PA organic moiety in agreement with the calculated value of 32.28%. In complex **III**, the decomposition reactions occur at two closed stages, observed at 196 and 647ºC which may be attributed to the loss of the donor and the acceptor organic moieties of the complex. The found and calculated weight loss values are in good agreements.

In complex **IV**, the decomposition reactions occur in two main stages and each one observed at two temperatures, 164, 251, 715, and 794ºC with a weight loss of 59.46 and 31.23%. These values of weight loss may be due to the loss of CFX and DDQ organic moieties in good agreement with the calculated values of 59.82 and 32.37%, respectively. In complex **V**, the decomposition reactions occur in two main stages at 200, 252, and 588ºC with a weight loss of 60.45 and 30.13%. These values of weight loss may be due to the loss of CFX and TCNQ organic moieties in good agreement with the calculated values of 61.83 and 30.10%, respectively [61].

Antibacterial activity. The antibacterial activity of the CFX complexes were screened in *vitro* against two gram-positive bacterial strains, *Staphylococcus aureus* and *Bacillus subtilis*, and two gram-negative bacterial strains, *Escherichia coli* and *Pseudomonas aeruginosa*. The tested CT-complexes were dissolved in DMSO to obtain 100 μg/mL stock solutions. The activity was determined by measuring the inhibition zone diameter

Table 7. Antibacterial activity for the CT-complexes of CFX

Sample	Inhibition zone diameter, mm			
	Bacillus subtillis, G^+	*Staphylococcus aureus*, G^+	*Escherichia coli,* G^-	*Pseudomonas aeroginosa*, G^-
DMSO	0.0	0.0	0.0	0.0
Ampicilin	20	18	22	17
I	14	16	15	14
II	15	15	18	15
III	14	16	15	15
IV	15	16	15	14
V	15	17	16	16

values (mm) of the complexes against the microorganisms. Ampicillin was used as the positive control. The screening data are listed in Table 7. The results indicated that the CFX CT-complexes exhibited moderate inhibitory results against all of the gram-positive and gram-negative bacterial species. It is obvious that the antibacterial activity of the CFX CT-complexes are lower than Ampicillin standard and complex **IV** have the higher antibacterial activity than other complexes.

CONCLUSIONS

Charge transfer interactions between the donor (CFX) and the σ-acceptor like I_2 and π-acceptors as HPA, H_2CA, DDQ and TCNQ were studied in MeOH at 25ºC. The synthesized CT-complexes were characterized using various spectroscopic techniques including UV–visible, IR and ^{1}HNMR spectroscopy and confirmed by elemental and thermal analyses. The reactions stoichiometries were found to be 1 : 1 for all complexes and had the formulas: $[(CFX)_2I]^+\cdot I_3^-$ (**I**), $[(HCFX)^+(PA)^-]$ (**II**), $[(HCFX)^+(HCA)^-]$ (**III**), $[(CFX_{-H})^-\cdot(HDDQ)^+]$ (**IV**), and $[(CFX_{-H})^-(HTCNQ)^+]$ (**V**). Reaction of CFX with iodine resulted in formation of tri iodide. The interaction between the donor (CFX) and HPA, H_2CA acceptors was due to transfer of proton from acceptor to nitrogen atom of donor to make hydrogen bonding, where the interaction mode between CFX and the DDQ, TCNQ acceptors occur through the migration of the H^+ ion from the NH_2 in CFX to one of the cyano groups in the DDQ and TCNQ acceptors to form a positive ion ($-C\equiv N^+-H$) that associates with the anion to form ion pairs. The obtained complexes are thermally stable. Physical parameters such as (K_{CT}, ε_{CT}, μ, ΔG, I_D, f, E_{CT}) and antibacterial activities have been estimated.

Finally, we could conclude that the interaction of Cefotaxime sodium (CFX) as a donor with different acceptors proceeds in a molar ratio of 1 : 1 according to Scheme 3.

REFERENCES

1. Roy, T, Dutta, K., Nayek, M.K., Mukherjee, A.K., Banerjee, M., and Seal, B.K., *J. Chem. Soc., Perkin Trans. 2*, 1999, p. 531.
2. Fla, F.P., Palou, J., Valero, R., Hall, C.D., and Speers, P., *J. Chem. Soc., Perkin Trans. 2*, 1991, p. 1925.
3. Roy, D.K., Saha, A., and Mukherjee, A.K., *Spectrochim. Acta A*, 2005, vol. 61, p. 2017.
4. Slifkin, A.M., *Charge-Transfer Interaction of Biomolecules,* New York: Academic Press, 1971.
5. Dozal, A., Keyzer, H., Kim, H.K., and Wang, W.W., *Int. J. Antimicrob. Agent.,* 2000*,* vol. 14*,* p. 261.
6. Korolkovas, A., *Essentials of Medical Chemistry,* New York : Wiley, 1998, *2* ed*.,* ch. 3.
7. Abou Attia, F.M., *Farmaco,* 2000*, 55,* p. 659.
8. Basavaiah, K., *Farmaco*, 2004, 59, p. 315.
9. Saleh, G.A., Askal, H.F., Radwan, M.F., and Omar, M.A., *J. Talanta*, 2001, vol. 54, p. 1205.
10. Salem H., *J. Pharm. Biomed. Anal*., 2002, *29*, p. 527.

11. Pandeeswaran, M., El-Mossalamy, E.H., and Elango, K.P., *Int. J. Chem. Kinet*., 2009, vol. 41, p. 787.
12. Pandeeswaran , M. and Elango, K.P., *Spectrochim. Acta A,* 2010, vol. 75, p. 1462.
13. Yakuphanoglu, F. and Arslan, M., *J. Solid State Commun*., 2004, vol. 132, p. 229.
14. Yakuphanoglu, F. and Arslan, M., *J. Opt. Mater.,* 2004, vol. 27, p. 29.
15. Yakuphanoglu, F., Arslan, M., Kucukislamoglu, M., and Zengin, M., *J. Sol. Energy.*, 2005, vol. 79, p. 96.
16. Chakraborty, B., Mukherjee, A.S., and Seal, B.K., *Spectrochim. Acta A,* 2001, vol. 57, p. 223.
17. Krishnamurthy, M., Surendrababu, K., and Muralikrishna, U., *Indian J. Chem. A*, 1988, vol. 27, p. 669.
18. Andrade, S.M., Costa, S.M.B., and Pansu, R., *J. Colloid Interface Sci.,* 2000, vol. 226, p. 260.
19. Dabestani, R., Reszka, K.J., and Sigman, M.E., *J. Photochem. Photobiol A.,* 1998, vol. 117, p. 223.
20. Jakubiak, R., Bao, Z., and Rothberg, L., *Synth. Met.*, 2000, vol. 114, p. 61.
21. Takahasi, K., Horino, K., Komura, T., and Murata, K., *Bull. Chem. Soc. Jpn.*, 1993, vol. 66, p. 733.
22. Eychmuller, A. and Rogach, A.L., *Pure Appl. Chem.,* 2000, vol. 72, p. 179.
23. Brueggermann, K., Czernuszewicz, R.S., and Kochi, J.K., *J. Phys. Chem.,* 1992, vol. 96, p. 4405.
24. Das, S.K., Krishnamoorthy, G., and Dofra, S.K., *Can. J. Chem.*, 2000, vol. 78, p. 191.
25. Jones, G. and Jimenez, J.A.C., *Tetrahedron Lett.*, 1999, vol. 40, p. 8551.
26. Smith, G., Lynch, D.E., Byriel, K.A., and Kennard, C.H.L., *J. Chem. Crystallogr.*, 1997, vol. 27, p. 307.
27. Smith, G., Lynch, D.E., and Bott, R.C., *Aust. J. Chem.*, 1998, vol. 51, p. 159.
28. Smith, G., Bott, R.C., Rae, A.D., and Willis, A.C., *Aust. J. Chem.,* 2000, vol. 53, p. 531.
29. Hamed, M.M.A., Abdel-Hamid, M.I., and Mahmoud M.R., *Monatsh. Chem.,* 1998, vol. 129(2), p. 121.
30. Mulliken, R.S., *J. Am. Chem. Soc.,* 1950, vol. 72, p. 600.
31. Foster, R., *Charge-Transfer Complexes*, London: Academic Press, 1969.
32. O'Neil, M.J., *The Merck Index, Merck Co Inc.,* New York: Whitehouse Station, 2006, 14 ed., p. 317.
33. Jones, R.N., *Infection.*, 1994, vol. 22, Supplement 3, p. 152.
34. Gentry, L.O., *Am. J. Med.,* 1990, vol. 88(4), p. 32.
35. *The Indian Pharmacopoeia*, New Delhi: The Controller of Publications, 1996, p. 148.
36. Raddatz, J.K., Ostergaard B.E., and J.C. Rotschafer, *Diagn. Microbiol. Infect. Dis.,* 1995, vol. 22, nos. 1–2, p. 77.
37. Gaballa, A.S., *Indian J. Chem.,* 2005, 44A , p. 1372; Gaballa, A.S., Wagner, C., Nour, E.M.,. Teleb, S.M, Elmosallamy, M.A.F., Kaluderovic, G.N., and Schmidt, H., and Steinbon D., *J. Mol. Struct.*, 2008, vol. 876, p. 301.
38. Gaballa, A.S., *J. Mol. Struct.*, 2013, vol. 1043, p. 91; Ali, M.M., Gaballa, A.S., Haggam, R.A, El-Khososy, N.A., and Teleb, S.M, *J. Chem. Pharm. Research.,* 2014, vol. 6(11), p. 570.
39. Skoog, D.A., *Principles of Instrumental Analysis,* New York: Saunder College Publishing, 1985, 3 ed, ch. 7.
40. Beecher, D.J. and Wong, A.C., *Appl. Microbiol.,* 1994, vol. 60, p. 4614.
41. *Methods for Antimicrobial Susceptibility Testing of Anaerobic Bacteria*, Approved Standard M11 A3.NCCLS, Wayne, PA, USA, 1993.
42. Gaballa, A.S., Teleb, S.M., Rusanov, E., and Steinborn, D., *J. Inorg. Chim. Acta*, 2004, vol. 357, p. 4144.
43. Al-Qaradawi, S.Y., Bazzi, H.S., Mostafa, A., and Nour, E.M., *J. Mol. Struct.,* 2011, vol. 998, p. 126.
44. Abou-Ettah, R. and El-Korashy, A., *J. Phys. Chem.,* 1972, vol. 76, p. 2405.
45. Tsubomura, H. and Lang, R.P., *J. Am. Chem. Soc.*, 1961, vol. 83, p. 2085.
46. Rathore, R., Lindeman, S.V., and Kochi, J.K., *J. Am. Chem. Soc.*, 1997, vol. 119, p. 9393.
47. Aloisi, G. and Pignataro, S., *J. Chem. Soc., Faraday Trans.,* 1972, vol. 69, p. 534.
48. Briegleb, G., *Z. Angew. Chem.,* 1960, vol. 72, p. 401; Briegleb, G., *Z. Angew. Chem.,* 1964, vol. 76, p. 326.
49. Abu-Eittah, R., and Al-Sugeir F., *Can. J. Chem.*, 1976, vol. 54, p. 3705.
50. Hassouna, M.E.M. and Zaki G.A.. *Int. J. Adv. Research.,* 2014, vol. 2(4), p. 453.
51. Al-Ahmary, K.M., Habeeb. M.M., and Al-Solmy, E.A., *J. Mol. Liqs.,* 2011, vol. 162, p. 129.
52. Al-Attas, A.S., Habeeb, M.M., and Al-Raimi, D.S., *J. Mol. Struct.* , 2009, vol. 928, p. 158.
53. Adam, A.A., *Spectrochim. Acta A,* 2013, vol. 104, p. 1.
54. Gaballa, A.S., Teleb, S.M., and Nour, E., *J. Mol. Struct.,* 2012, vol.1024, p. 32.

55. Muhtadi, F.J., *Anal. Profiles Drug Subst.*, 1984, vol. 13, p. 737.

56. Mayo, D.W., Miller, F.A., and Hannah, R.W., *Course Notes on the Interpretation of Infrared and Raman Spectra*, John Wiley & Sons, 2003; Stuart, B.*, Infrared Spectroscopy: Fundamentals and Applications,* John Wiley & Sons, Ltd, 2004; Azeem, S.W., Khan, M.A., and Ahmad, I., *Pak. J. Pharm. Sci.,* 2005, vol. 18, p. 33.

57. Singh, N. and Ahmad, A., *J. Mol. Struct.,* 2010, vol. 977, p. 197.

58. Teleb, S.M. and Gaballa, A.S., *Spectrochim. Acta Part A.*, 2005, vol. 62, nos. 1–3, p. 140.

59. Mitchell, T.N. and Costisella, B., *NMR – From Spectra to Structures*, *An Experimental Approach,* Berlin: Springer, 2007, 2 ed.

60. Lounasmaa M. and Tolvanen A, *Heterocycles.,* 1988, vol. 23, p. 372.

61. *Thermal Analysis of Micro, Nano-and Non-Crystalline Materials,* Šesták, J. and Šimon, P., Eds.*,* Springer Science+Business Media Dordrecht, 2013.